Deformation of ferrofluid marbles in the presence of a permanent magnet

Nam-Trung Nguyen

Queensland Micro- and Nanotechnology Centre, Griffith University, Brisbane, 4111, Australia.

KEYWORDS. Liquid marble, ferrofluid, droplet, micro magnetofluidics, digital microfluidics

ABSTRACT. This paper investigates the deformation of ferrofluid marbles in the presence of a permanent magnet. Ferrofluid marbles are formed using a water-based ferrofluid and 1-µm hydrophobic polytetrafluoride particles. A marble placed on a Teflon coated glass plate deforms under gravity. In the presence of a permanent magnet, the marble is further deformed with a larger contact area. The geometric parameters are normalized by the radius of an undistorted spherical marble. The paper first discusses a scaling relationship between the dimensionless radius of the contact area as well as the dimensionless height and the magnetic Bond number. The dimensionless contact radius is proportional to the fourth root of the magnetic Bond number. The dimensionless height scales with the inverse square root of the magnetic Bond number. In the case of a moving marble dragged by a permanent magnet, the deformation is evaluated as the difference between advancing and receding curvatures of the top view. The dimensionless height and the contact diameter of the marble do not significantly depend on the speed or the capillary number. The scaling analysis and experimental data show that the deformation is proportional to the capillary number.

Introduction

Micro magnetofluidics is an emerging research area examining and exploiting the interactions between magnetism and fluid on the microscale.[1] Magnetism provides a convenient way to induce a body force to a fluid in the microscale. For instance, a varying magnetic body force can tune the shape of a sessile droplet, which usually is determined by gravity and surface tension.[2] A magnetic fluid consists of a carrier fluid and a suspension of magnetic particles. If the magnetic particles are smaller than about 10 nm, the thermal energy dominates over the magnetic energy. With support of surfactants, the nanoparticles can disperse homogenously in the carrier fluid. The whole fluid behaves as a paramagnetic liquid and is called ferrofluid. Recently, we demonstrated that a ferrofluid droplet can work as a vehicle for transporting discrete diamagnetic droplets in digital microfluidics.[3]

To reduce wetting and friction of a sessile droplet, the surface of a digital microfluidic platform needs a hydrophobic coating. The viscous loss caused by the sliding motion of the droplet requires a relatively large amount of energy from the actuation scheme. A rolling motion can reduce this loss.[4] Rolling motion is possible if the surface is super hydrophobic or the liquid droplet is coated with hydrophobic particles. The liquid droplet of the latter case is called a liquid marble.[5] Liquid marbles were originally obtained by mixing hydrophobic powder with water.[6] Due to the hydrophobic nature of the powder, the grains do not dissolve into water but stay on the droplet surface, forming a coating layer. Parameters such as density, particle size, particle shape are critical to the successful formation of a liquid marble.[6]

Aussillious and Quere investigated in details the properties of stationary and moving liquid marbles.[7] Similar to a sessile droplet, the static shape of a marble under gravity has two basic

forms: a sphere and a puddle. The Bond number Bo describes the relative ratio between gravitational energy and surface energy. A small liquid volume ($Bo \ll 1$) assumes a spherical shape due to the dominant surface tension. A large liquid volume ($Bo > 1$) has the shape of a puddle. The radius of the contact area between a spherical marble and the solid surface is proportional to the square root of the Bond number.[4,7] The puddle height is constant and can be used for estimating the relative surface tension of a liquid marble.[8,9,10]

A magnetic liquid marble can be controlled by an external magnetic field. This type of marbles is formed either by using hydrophobic magnetic particles as the coating[11-14] or by dispersing magnetic nanoparticles in the liquid[15]. Bormashenko reported preliminary results on using a magnet to drive marbles and droplets containing ferrofluid. However, the effect of the magnetic field on the shape of the ferrofluid marble were not reported. Recently, we investigated the deformation of a ferrofluid suspended in oil under a horizontal uniform magnetic field.[16] In this work, the effect of gravity and magnetic field are decoupled due to the different field directions. No generalized scaling law has been derived for the relationship between magnetic field and the deformation. Afkhami et al. investigated numerically and experimentally the deformation and the field-induced motion of a ferrofluid droplet suspended in a viscous medium.[17,18] Recently, Timonen et al. investigated static and dynamic self-assembly of magnetic droplets on super hydrophobic surfaces in the presence of large magnets.[19] The magnet diameter is one or two order of magnitudes larger than that of the droplet. This configuration leads to elongation, instability and splitting of the droplet and is not suitable for digital microfluidics. More recently, Piroird et al.[20] investigated the deformation of a Leidenfrost liquid oxygen droplet in the presence of a permanent magnet. This work utilized the relative distance between the droplet and the magnet to vary the magnetic force. Since the magnetic susceptibility of liquid

oxygen is about two orders of magnitude smaller than that of ferrofluid, a strong magnet with flux density of several Teslas was needed.

To the author's best knowledge, no detailed work has been reported on the effect of a magnetic field on stationary and moving ferrofluid marbles. Previous works only investigated the side-view deformation. Terminal velocity of a droplet or a marble moving down an inclined plane was investigated as the only kinematic behavior.[7] No previous works have been reported on the top-view deformation of a moving liquid marble.

One of the reasons for the missing works on a moving marbles is the availability of a suitable actuation scheme. All marbles under previous investigations were actuated by gravity. Actuation with gravity has little use in practical applications such as digital microfluidics. The recent work by Piroird et al.[20] derived the relationship between the velocity of a liquid oxygen drop and the deformation caused by a stationary magnet. Magnetic field strength was the only independent parameter of this experiment. Further, the volume of the liquid oxygen droplet cannot be accurately dispensed due to the required low-temperature condition. Our previous work on moving sessile ferrofluid droplets showed that a moving permanent magnet can provide well controlled field strength and moving speed for the deformation study.

The present paper provides a scaling analysis for geometric parameters such as the height and the contact radius. The paper also investigates the deformation of a moving ferrofluid marble in the presence of a linearly actuated permanent magnet. A simple scaling relationship is derived for the deformation represented by the difference between the advancing and receding curvatures. Actuation parameters are represented by dimensionless numbers such as capillary

number Ca and magnetic Bond number Bm. The scaling relationship was confirmed by experiments with marbles of different volumes and permanent magnets of various strengths.

Stationary Ferrofluid Marble

Radius of Contact Area

Figure 1(a) shows the schematic of a stationary ferrofluid marble. The scaling analysis follows the energy approach proposed by Mahadevan and Pomeau.[4] The spatial parameters are made dimensionless using the radius of the undistorted marble $R = \sqrt[3]{3V/4\pi}$, where V is the volume. The radius R is therefore used as the characteristic length scale in our analysis. The relative ratio between gravitational energy and surface energy is represented by the Bond number $\mathrm{Bo} = \rho g R^2/\sigma$, where ρ is the density and σ is the surface tension. The relative ratio between magnetic energy and surface energy is represented by the magnetic Bond number $\mathrm{Bm} = RMB/\sigma$, where M is the magnetization density of the ferrofluid in A/m, B is the magnetic flux density in Tesla (T, $\mathrm{kgs^{-2}A^{-1}}$). Under gravity and magnetic force, the center of mass of the marble is lowered by δ forming a circular contact area of a radius l. The contact radius l relates to the displacement of the center of mass as[4]

$$l^2 \sim R\delta \text{ or } \delta \sim l^2/R \qquad (1)$$

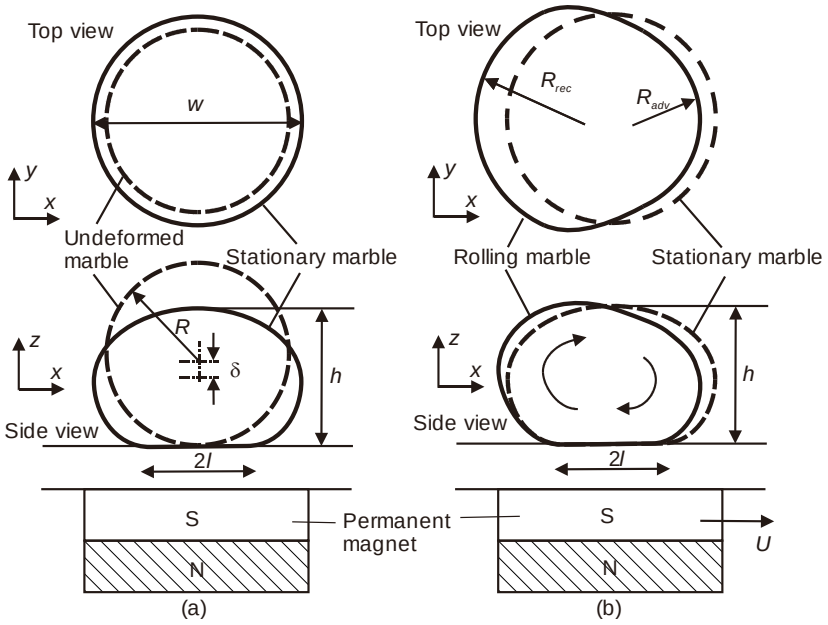

Fig. 1 Deformation of a ferrofluid marble with an original radius of *R*: (a) Under its own weight and the magnetic force induced by the permanent magnet, the marble deforms with a contact radius of *l*, a height *h* and a width *w*. (b) The marble is dragged by a permanent magnet moving with a constant linear speed. The marble deforms so that the receding end adopts a larger radius of curvature (not to scale).

The increase in surface energy is caused by the change in potential energy $\rho g R^3 \delta$ and the addition of the magnetic energy $R^3 MB$:

$$\rho g R^3 \delta + M R^3 B \sim \sigma l^4 / R^2 \qquad (2)$$

In the absence of a permanent magnet, the magnetic energy disappears in (2), leading to the scaling relationship as derived by Mahadevan and Pomeau[4]:

$$l \sim \mathrm{Bo}^{1/2} R \qquad (3)$$

or in the dimensionless form:

$$l^* = l/R \sim \mathrm{Bo}^{1/2} \qquad (4)$$

In the case of a large Bond number ($\mathrm{Bo} \geq 1$), the marble takes the shape of a puddle and the

contact radius scales with the fourth root of the Bond number[7]:

$$l^* \sim R^{1/2}\kappa^{1/2} = \mathrm{Bo}^{1/4} \quad (5)$$

where $\kappa^{-1} = \sqrt{\sigma/\rho g}$ is the capillary length.

Following the energy approach proposed by Bormashenko et al.[21], the ratio between the induced magnetic energy and the gravitational energy is:

$$\xi = \frac{MR^3B}{\rho g R^3 \delta} = \frac{MB}{\rho g \delta} \quad (6)$$

Since both magnetic and gravitational energies are volume-based, the above dimensionless number does not scale with the marble size. Taking the capillary length κ^{-1}as the characteristic length to replace the displacement in (6), a critical magnetic flux density for the case $\xi = 1$ can be derived as $B_{cr} = \sqrt{\sigma\rho g}/M$. For properties of the marbles in our investigation ($\sigma = 34 \times 10^{-3}$N/m, $M = 6 \times 10^3$A/m, $\rho = 1070$ kg/m^3), the critical magnetic flux density is $B_{cr} =$ 3.15 mT. Since the displacement of center of mass is always smaller than then the capillary length, the actual critical magnetic flux density is even smaller than this value.

If the magnetic flux density of the permanent magnet is much larger than the critical value ($B \gg B_{cr}$), the magnetic force is larger than the weight of the marble (Bm $\gg$ Bo). The negligible change in potential energy leads to:

$$MR^3B \sim \sigma l^4/R^2 \quad (7)$$

Inserting (1) into (7) results in:

$$MR^3B/\sigma \sim \delta^2 \quad (8)$$

$$\mathrm{Bm}R^2 \sim \delta^2 \sim l^4/R^2 \quad (9)$$

$$l \sim \mathrm{Bm}^{1/4}R \quad (10)$$

or in the dimensionless form:

$$l^* \sim \mathrm{Bm}^{1/4} \quad (11)$$

Height of the Marble

The scaling law for the height can be derived from the radius of contact area and the initial marble volume. For a small marble ($\mathrm{Bo} \ll 1$) without a permanent magnet, the height is approximately the diameter $2R$ of the marble,[7] The dimensionless height $h^* = h/R \approx 2$ is therefore constant. With a large Bond number ($\mathrm{Bo} \geq 1$), the marble takes a puddle shape with a constant height of $h = 2\kappa^{-1}$. Normalizing the height by the undistorted radius *R* leads to:

$$h^* = 2\mathrm{Bo}^{-1/2} \qquad (12)$$

In the presence of a permanent magnet with a large flux density ($B \gg B_{cr}$), the marble is flattened and the height of the marble can be estimated from the cylindrical shape as $h = V/\pi l^2$. Substituting the scaling relationship of (10) into the above formula, the dimensionless height of a ferrofluid marble in the presence of a permanent magnet scales as:

$$h^* \sim \mathrm{Bm}^{-1/2} \qquad (13)$$

Moving Ferrofluid Marble

If the permanent magnet moves with a linear speed of *U*, the marble will be dragged along with the same speed. Due to its hydrophobic nature, the marble moves with a combination of sliding and rolling similar to the case investigated by Aussillous and Quere.[7] In contrast to the previous works using an inclined plane, the speed of the marble now can be arbitrary determined by the speed of the magnet. Assuming a large viscosity ratio between the marble liquid and the surrounding air, the flattened marble further deforms in response to the viscous loss of the internal flow. The radii of curvature at the receding end become larger than that of the advancing end, Fig. 1(b). The relative ratio between viscous loss inside the marble and the surface tension is

represented by the capillary number $\mathrm{Ca} = \mu U/\sigma$, where μ is the dynamic viscosity of the marble liquid.

The Reynolds number $\mathrm{Re} = \rho U D_h/\mu$ represents the relative ratio between inertia and viscous loss, where D_h is the hydraulic diameter. Considering the deformed marble as a flat channel with high aspect ratio ($h \ll 2l$), the hydraulic diameter is approximately the height, $D_h \approx h$. In our experiments, Reynolds number is less than unity and the flow within the marble can be assumed as laminar. The friction force between the marble and the glass surface is balanced by the dragging magnetic force. Thus, the pressure drop between the receding advancing ends of the marble scales as:

$$\Delta P \sim \mu \frac{2l}{{D_h}^2} U = \mu \frac{2l}{h^2} U \qquad (14)$$

The difference in Laplace pressure between the advancing and receding ends of the marble is:

$$\Delta P = \sigma \left[\left(\frac{1}{R_{\mathrm{adv}}} - \frac{1}{R_{\mathrm{rec}}} \right)_{xy} + \left(\frac{1}{R_{\mathrm{adv}}} - \frac{1}{R_{\mathrm{rec}}} \right)_{xz} \right], \qquad (15)$$

where *xy* and *xz* are the respective imaged top-view and side-view planes of the marble. As observed later in the experiments, the marble is flattened leading to no significant difference between the radii of curvature in *xz*-plane, Fig. 1(b). From the energy point of view, the deformation prefers the geometry on the *xy*-plane, which is unrestricted by gravity and magnetic force. Thus, the difference of curvatures in the *xz*-plane can be neglected. Henceforth, the receding and advancing radii $R_{\mathrm{adv}}, R_{\mathrm{rec}}$ are meant for the *xy*-plane only. Introducing the difference in curvature:

$$\Delta R^{-1} = \frac{1}{R_{\mathrm{adv}}} - \frac{1}{R_{\mathrm{rec}}} \qquad (16)$$

and balancing the hydrodynamic pressure and Laplace pressure lead to:

$$\mu\frac{2l}{h^2}U\sim\sigma\Delta R^{-1} \qquad (17)$$

Using the radius R of the undistorted marble, the length, the height and the difference in curvature are made dimensionless as $h^*=\frac{h}{R}, l^*=\frac{l}{R}, (\Delta R^{-1})^*=\Delta R^{-1}\cdot R$. The scaling relationship of (17) then has the form:

$$(\Delta R^{-1})^*\sim\frac{\mu U}{\sigma}l^*h^{*-2}=\mathrm{Ca}l^*h^{*-2} \qquad (18)$$

Assuming the pulling effect of the magnet on the geometry of *xz* plane is the same as for the stationary case, the two asymptotic cases for the scaling relation (18) are:

$$\begin{cases} l^*\sim\mathrm{Bm}^{1/4} \\ h^*\approx 2 \end{cases} \text{ for a semi-spherical shape} \qquad (19)$$

$$\begin{cases} l^*\sim\mathrm{Bm}^{1/4} \\ h^*\sim\mathrm{Bm}^{-1/2} \end{cases} \text{ for a puddle shape} \qquad (20)$$

Substituting (19) and (20) into (18) leads to the scaling relation for the deformation of the moving marble:

$$(\Delta R^{-1})^*\sim\mathrm{CaBm}^{1/4} \text{ for a semi-spherical shape} \qquad (21)$$

$$(\Delta \boldsymbol{R^{-1}})^*\sim\boldsymbol{\mathrm{CaBm}^{5/4}} \text{ for a puddle shape} \qquad (22)$$

Materials and Method

Polytetrafluorethylene (PTFE) particles (Sigma-Aldrich) was used to form the marble. The PTFE particles have a size of 1 μm and a density of 2150 kg/m^3. Water-based ferrofluid EMG-508 was purchased from Ferrotec Corporation (USA). The 10-nm Fe_3O_4 nanoparticles in the ferrofluid

has a volume concentration of 1.8 %. A surfactant helps to keep the nanoparticles apart from each other. The dynamic viscosity at 27°C is μ=5 mPas. The density at 25°C is ρ=1.07 g/cm^3. The initial susceptibility is χ=0.24. A surface tension σ=31.7±0.05 mN/m of the ferrofluid was measured with a commercial tensiometer (TVT-2, measurement range of 0.1 to 100 mN/m, error of ±0.01-0.05 mN/m, Lauda, Germany). The measured surface tension is lower than the value of 53mN/m given by the vendor. A micropipette (Finnpipette, Thermo Scientific) was used to dispense small volumes of ferrofluid ranging from 0.5 µl to 10 µl. For volumes greater than 10 µl, the dispensing process was repeated until the required volume is achieved.

The hydrophobic PTFE powder was first spread on a Petri dish. The required volume of the ferrofluid was subsequently dispensed by the micropipette on a bed of PTFE powder. The ferrofluid droplet was then rolled until the whole droplet is covered with PTFE microparticles. As later observed under the camera setup, marbles with a volume larger than 50 µl assumes a puddle form with a constant height of 3.6 mm. This height is used for estimating the effective marble surface tension of $\sigma = \rho g h^2/4 = 34.0$ mN/m. This value is slightly higher than the measured value. This estimated effective surface tension will be used for the evaluation of subsequent experimental data. The corresponding capillary length and the critical radius of the marble are $\kappa^{-1} = R_{\mathrm{cr}} = 1.8$ mm. Thus the volume for an unity Bond number (Bo=1) is $V_{\mathrm{cr}} = \frac{4}{3}\pi {R_{\mathrm{cr}}}^3 = 24.4$ µl, which is in the middle of the range investigated in our experiments. In our experiments, the surface tension and gravitational energies are on the same order of magnitudes but one or two order of magnitudes smaller than magnetic energy.

The same experimental setup of our previous work[2] was used for the characterization of the ferrofluid marbles. Images of the marble were captured by a CCD camera (Pulnix, progressive scan camera, JAI Inc., Japan) and the corresponding camera software (Video Savant

3.0, IO Industries, Ontario, Canada). The top view and side view were captured in a single image using a gold coated 45° prism mirror (Edmund Optics, USA). Figure 2(a) shows the side view of the marbles without a permanent magnet.

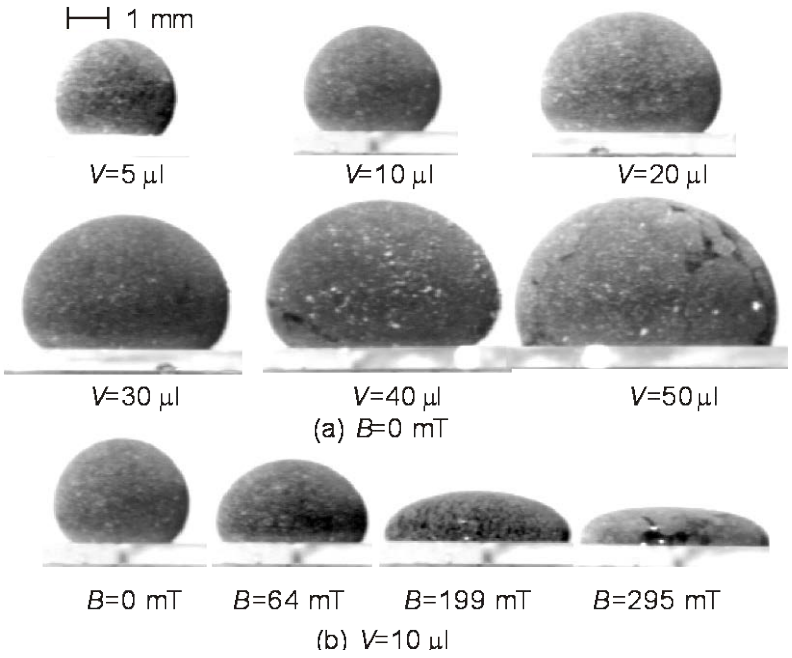

Fig. 2 Shapes of ferrofluid marbles: (a) Different volumes in the absence of a permanent magnet; (b) 10-μl ferrofluid marbles in the presence of permanent magnets with different strengths.

The magnetic field strength was varied using different nickel plated neodymium disc magnets (Eclipse Magnetics, UK). A gaussmeter GM05 (Hirst Magnetics Instruments Ltd) was used to measure the actual flux density on the surface of the magnet. The fabrication of the Teflon coated glass plate was reported previously.[2] The magnet is placed directly below the glass plate and a plastic ruler. The magnetic strength measured on the surface of the small (diameter of 3 mm, height of 2 mm), medium (diameter of 6 mm, height of 6 mm) and large (diameter of 10 mm, height of 5 mm) magnets are 64 mT, 199 mT and 295 mT respectively. Figure 2(b) shows the side view of a 10-μl marble in the presence of the different magnets. These values are

one to two orders of magnitude larger than the critical magnetic flux density $B_{cr} = 3.15$ mT. Thus, relative to magnetism, gravity is negligible in our experiments.

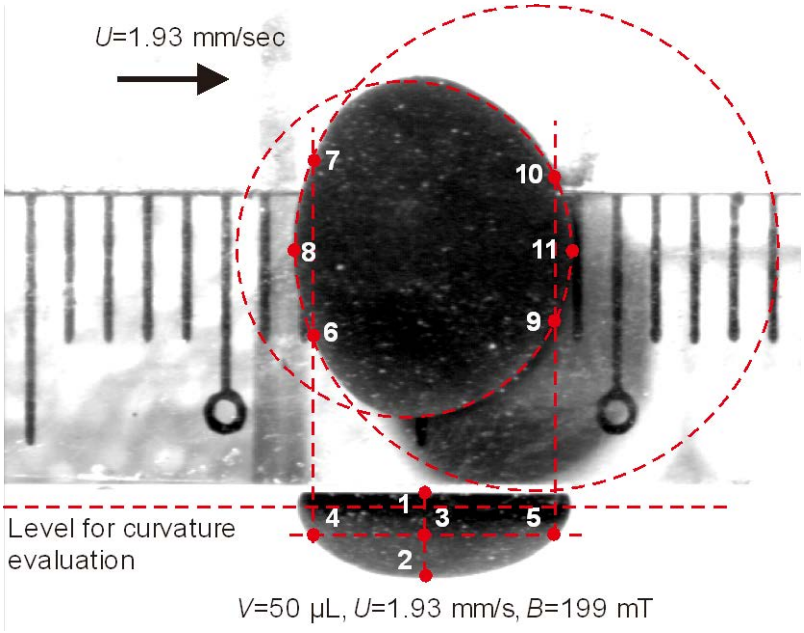

Fig. 3 The deformation of a moving ferrofluid marble.

The magnets were positioned on a programmable syringe pump. The speeds were adjusted by the programmed flow rates and converted to the linear speed. The speeds were later confirmed by direct evaluation of the recorded images. The speed values used in our experiments were 0.577, 0.770, 0.962, 1.16, 1.35, 1.54, 1.73 and 1.93 mm/sec. The recorded images were evaluated by a customized program written in Matlab (Mathworks, USA) using image processing tools. To prevent error propagation, all geometric parameters such as height, contact diameter and radii of curvature were measured and evaluated in pixel first and converted to SI unit in the final stage. For each data point, a mean value and standard deviation were evaluated using 12 different images. For consistency, the advancing and receding radii of curvature were measured by three-point fitting of the curvature with the procedure depicted in Fig. 3. Points 1 and 2 across the

maximum height of the marble is first determined. A line is drawn perpendicular to and at the middle 3 of line 1-2, cutting the receding and advancing ends at points 4 and 5. Points 4 and 5 are projected to the top view (*xy*-plane) to get the base of the sectors 6-8-7 and 9-11-10. Points 8 and 9 are selected at the tips of the two ends. The radii of the circles passing through 6,7,8 and 9,10,11 are subsequently determined.

Results and Discussion

Stationary Ferrofluid Marble

Figure 2(a) shows the side-view images of the 6 marbles with different volumes under investigation. The Bond numbers of these marbles ranges from 0.347 to 1.61. Clear deviation from the spherical shape can be observed with marbles of a volume of 10 μl and larger.

In the presence of a permanent magnet, the magnetic force pulls the marble to the surface, Fig. 2(b). The strong deformation and the increasing surface area may cause cracks in the hydrophobic coating. If the cracks are not in the contact area, the marble shape is not affected due to similar values of surface tension of the ferrofluid and the marble. If the cracks are in the vicinity of the contact area at the base, ferrofluid may partially wet the solid surface and destroy the marble.

The contact diameter and the height of the different marbles were first evaluated. The depicted data are coded as follow. White circles depict the data without a permanent magnet. Red circles depict data of the 64-mT magnet. Blue squares depict data of the 199-mT magnet. Green diamonds depict the data of the 295-mT magnet. Figure 4(a) and 4(b) show the measured data of the width w of the marble and the diameter $2l$ of the contact area. As the marble is flattened under higher magnetic flux densities and assumes the puddle shape, the width w

approaches the value of the diameter 2*l* of the contact area. In the absence of the permanent magnet, the diameter is smaller than the width. At the volume of 50 µl, the apparent change to the puddle shape leads to a jump of the diameter, Fig. 4(b).

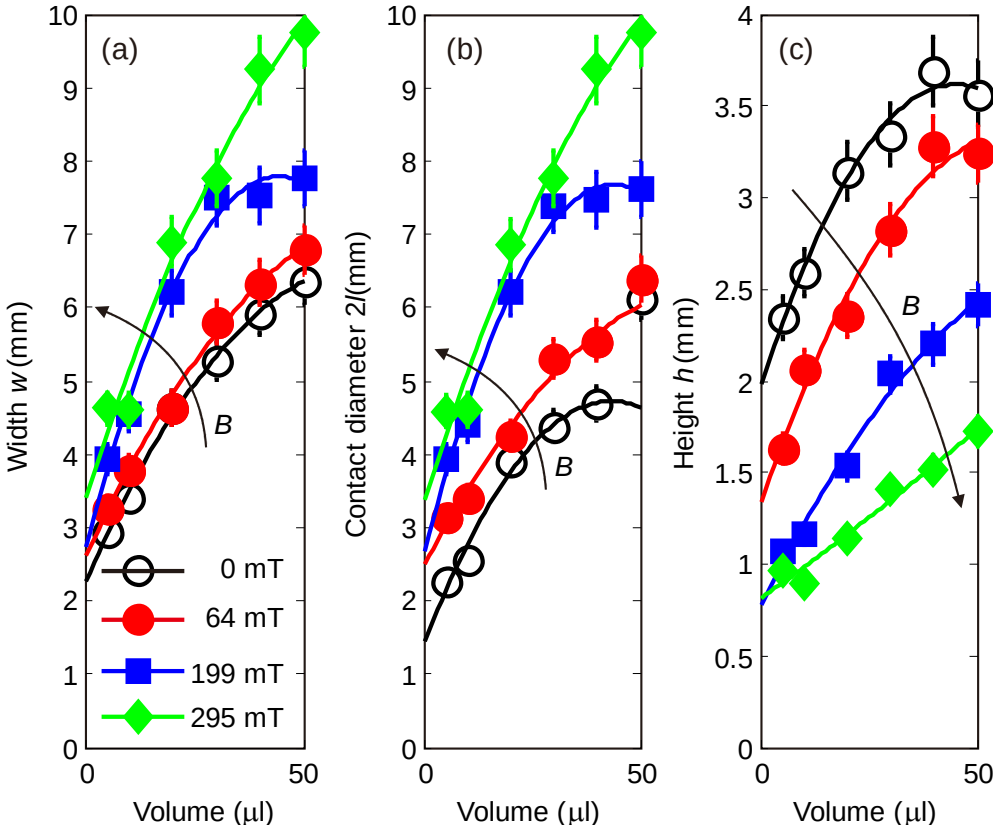

Fig. 4 Deformation of stationary ferrofluid marbles: (a) width *w* ; (b) diameter of contact area 2*l*; (c) height *h*

Figure 4(c) shows the measured height of the marbles at different magnetic flux densities. Data of at least three marbles were collected for each data point. Data in pixels were converted into millimetres using the ruler markings as reference. The general trend of decreasing height with increasing flux density can be observed.

To validate the scaling analysis for dimensionless contact radii and heights, the data depicted in Figure 4 are normalized and plotted against the corresponding Bond numbers and

magnetic Bond numbers. For the calculation of the magnetic Bond number, the magnetic flux density B is assumed to be that measured at the surface of the magnet. However, the base of the ferrofluid marble is separated by about 1 mm away from the magnet. The actual value of B is therefore lower. This smaller value can be taken care of by a proportional factor. The scaling power law is then still valid. The magnetization density of the ferrofluid depends on the applied field strength or the flux density. Since the magnetization data of the ferrofluid EMG-508 is not available, we assume that the ferrofluid is saturated and have an estimated value of M=6000 A/m, similar to that of the ferrofluid EMG-707.[12]

Figure 5(a) shows the dimensionless contact radius of the ferrofluid marbles versus Bond numbers (white circles, without magnet) and versus magnetic Bond numbers (solid points, with magnet). Without a magnet, the trend of the data indicates that the ferrofluid marbles follow the behavior of a puddle. The only outlier is the data point of the 5-μl marble. This conclusion agrees well with the observable deformation of the marbles larger than 10 μl, Fig. 2(b). In the presence of a permanent magnet, the magnetic force is significantly larger than the gravitational force leading to a magnetic Bond number Bm one to two orders of magnitude larger than the Bond number Bo. As predicted from the scaling analysis, the contact radius scales with the fourth root of the magnetic Bond number. The proportional factors of the fitting curves for both cases are of the same order of magnitude (1.1 and 0.6) indicating that magnetic field and gravity field affects the shape of a ferrofluid marble in the same manner.

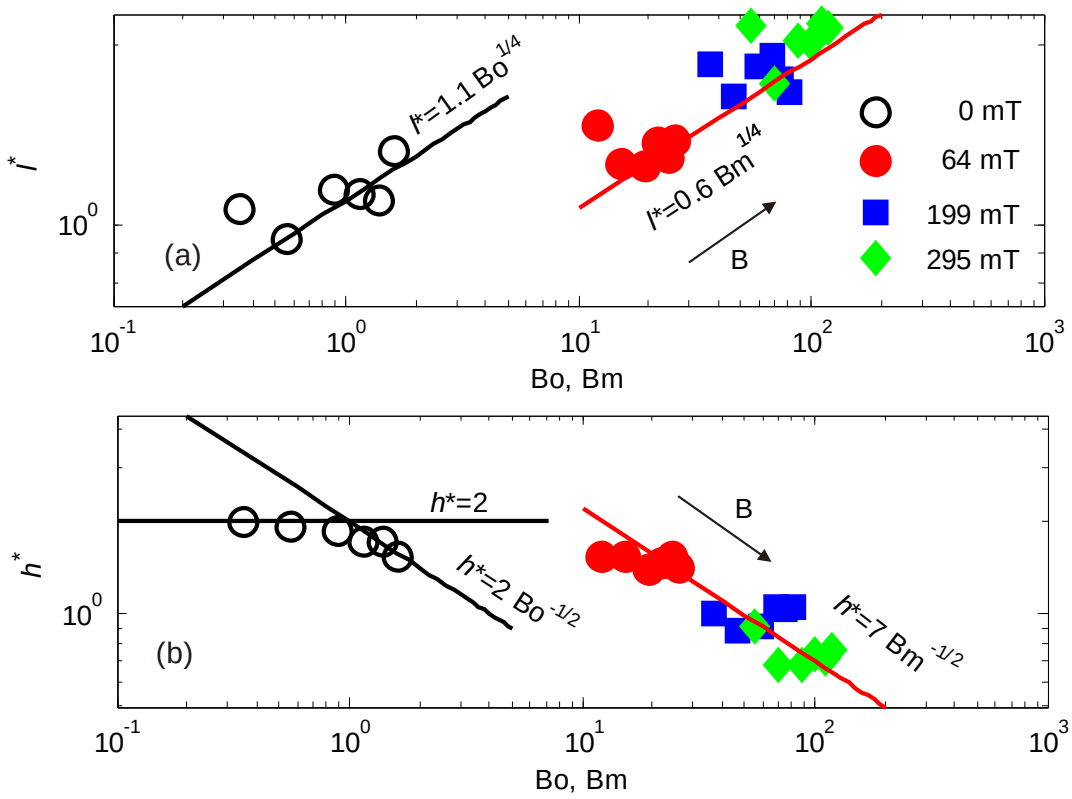

Fig. 5 Dimensionless parameters of stationary ferrofluid marbles versus Bond number Bo and magnetic Bond number Bm: (a) contact radius; (b) height.

Figure 5(b) depicts the dimensionless height of the ferrofluid marbles versus Bond number and magnetic Bond number. In the absence of a permanent magnet, the dimensionless height of Bond numbers larger than 1 follows the scaling law of a puddle shape ($h^* = 2\mathrm{Bo}^{-1/2}$). For Bond numbers smaller than 1, the dimensionless height approaches the value of a spherical shape (h^*=2). In the presence of a permanent magnet, the dimensionless height follows the inverse square-root scaling relationship of equation (13).

A common observation made with Figure 5 is that the data of magnetic deformation is on the right of those of gravimetric deformation. The reason may be the overestimated magnetic Bond number. The ferrofluid marble is actually about 1 mm apart from the magnet surface. The

field strength decreases further along the height of the marble. Thus, the actual magnetic flux density and the actual magnetic Bond number experienced by the marble are smaller. Therefore, the actual data of magnetic deformation may shift further to the left and align with the data of gravimetric deformation.

Moving Ferrofluid Marble

Figure 6 shows the dimensionless height and contact diameter of marbles with different magnets and speeds. The standard deviations caused by the different volumes are represented by the error bars. The fitting lines are estimated using the fitting functions from Fig. 5 and a magnetic Bond number representative for each magnet. In general, the dimensionless height and contact length remains almost constant with increasing speed or capillary numbers. This observation confirms the hypothesis that there is no significant change in the side view (*xz*-plane) between the stationary state and the moving state. The relatively large magnetic Bond number determines the height and the contact diameter of the marble. A small magnetic Bond number and a high capillary number, viscous loss and surface energy may be on the same order of magnetic energy leading to a slight but noticeable decrease in dimensionless height, Fig, 6(a). The results show that the capillary number of the moving marble is on the order of 10^{-4}, the corresponding Weber numbers ($\mathrm{We} = \rho U^2 R/\sigma$) are on the order of 10^{-5}. These small values indicate that both viscous and inertial effects are smaller than the surface effect allowing the marble to keep its quasi-static shape in *xz*-plane.

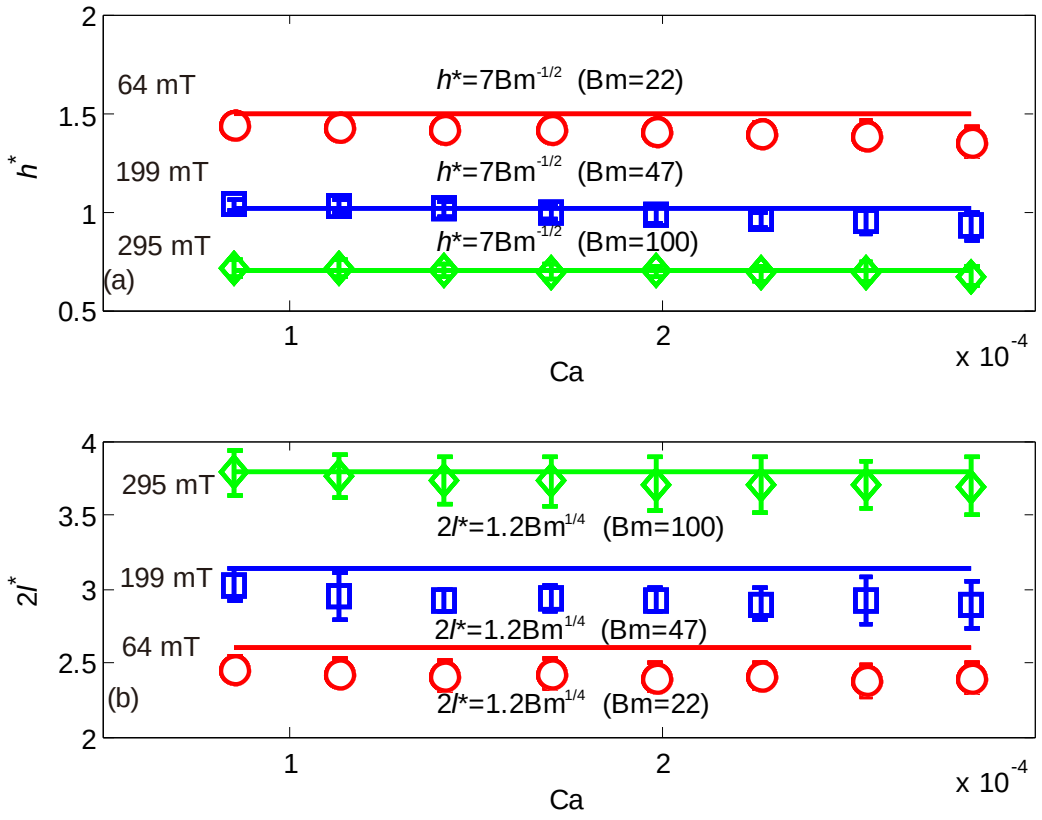

Figure 6 Dimensionless height (a) and contact diameter (b) of the marbles as function of capillary numbers.

Figure 7 depicts the same set of data versus the magnetic Bond number. The fitting lines indicate that the dimensionless height and contact diameter generally follow the scaling relationship of a stationary marble. Figure 7(a) shows that all marbles are flattened by the magnets and the height is smaller than the ideal case of a perfect sphere with $h^* = 2$. The vertical spreads in the data of Fig. 7(a) are from data of small marbles (low magnetic Bond number) and high speeds (high capillary number).

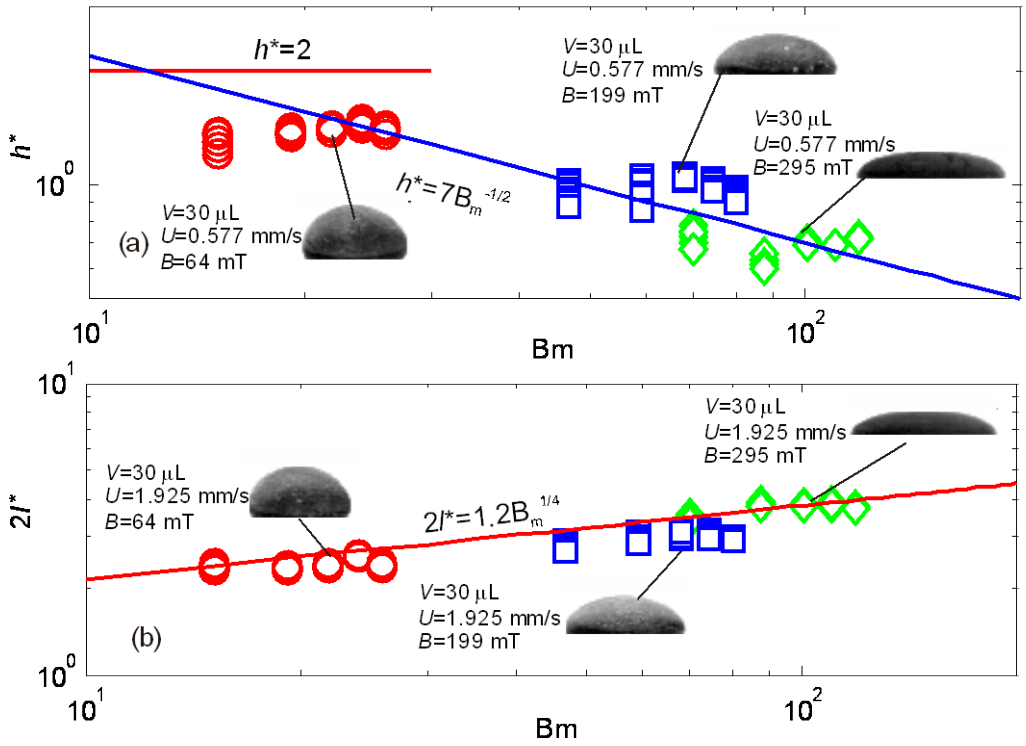

Fig. 7 Dimensionless parameters of moving ferrofluid marbles versus Bond number Bo and magnetic Bond number Bm: (a) height; (b) contact diameter.

The absence of vertical spread in the data of Fig. 7(b) confirms that the contact diameter does not change significantly with capillary number. The data scale well with the fourth root of the magnetic Bond number. The results of Fig. 7 validate the hypothesis that in response to the viscous loss at high capillary numbers, the marble rather deforms in the top-view *xy*-plane than in the side-view *xz*-plane. Examples of the side view of the marble are shown as inserts in Figure 7. No significant difference between advancing and receding ends of the marble can be observed.

As discussed above, small marbles with low magnetic Bond number are more sensitive to speed and capillary number. Thus, a 10-μL marble was used to evaluate the influence of capillary number on advancing and receding curvatures, Figure 8.

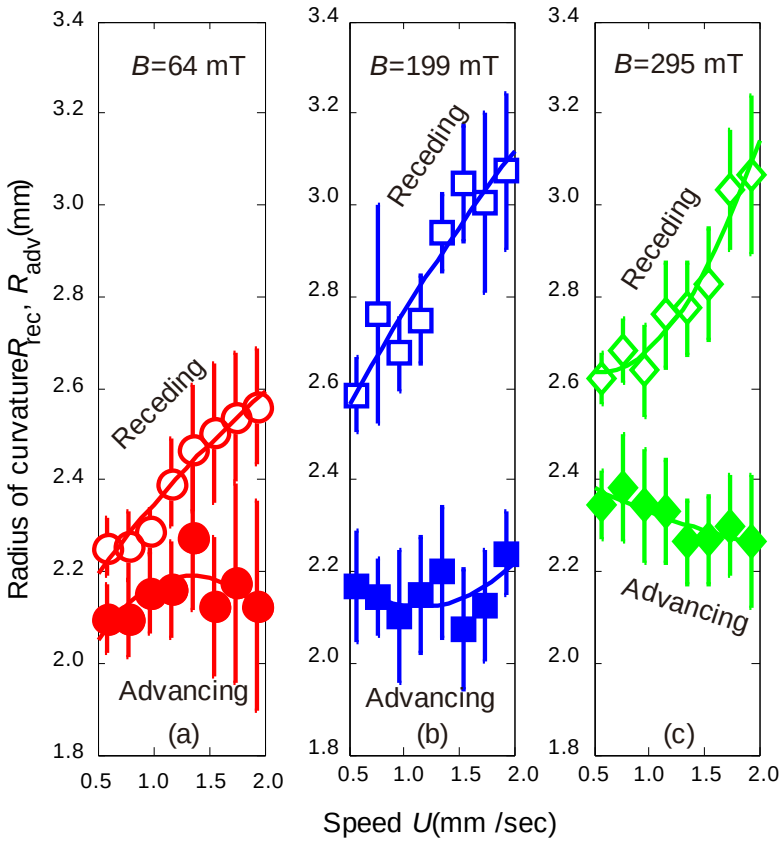

Figure 8 Measured receding and advancing radii of curvature of a 10-μL marble as function of speeds with different magnetic strengths.

The results show that while the advancing curvature remains almost constant, the receding curvature responds to the increasing speed. Compared to the 64-mT and 199-mT magnets, the difference between the receding and advancing radius of curvature of the 295-mT magnet is reduced, Fig. 8(c). Due to the stronger magnetic force and the extremely flattened shape, the assumption of the decoupling between the deformation in the *xy*-plane and the magnetic force may no longer holds. Figure 9 depicts the dimensionless change in curvature $(\Delta R^{-1})^*$ versus the capillary number.

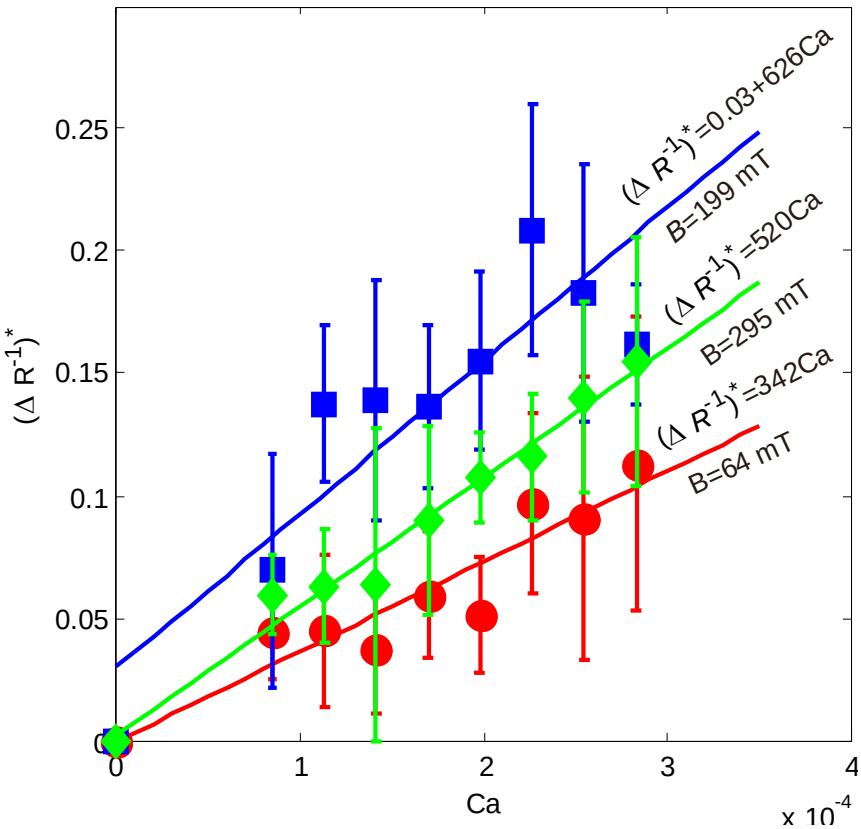

Figure 9 Measured dimensionless change in curvature $(\Delta R^{-1})^*$ of a 10-μL marble as function of capillary number at different magnetic strengths.

The results generally confirm the predicted linear relationship between the dimensionless change in curvature and the capillary number (21) and (22). With the 199-mT magnet, cracks appear on the coating causing the ferrofluid at some areas of the marble to contact directly with the solid surface. This behavior causes the data to spread and the offset in the fitting line, Fig. 9. The smaller slope of the 295-mT magnet indicates that the deformation on the *xy*-plane is strongly affected by the large field strength or a large magnetic Bond number. Even with the presence of cracks on the coating, the strong magnetic force leads to a smooth motion and a better fit to the scaling relationship. Our current experiment design cannot separate the influence of the volume and the magnetic field strength from the overall magnetic Bond number. Furthermore, the investigated volumes are around the critical case of Bo=1, so that the influence

of gravity cannot be isolated. Therefore, the scaling relationship with magnetic Bond number (21, 22) cannot be validated conclusively by the present experimental data.

Conclusions

The paper reports a scaling analysis for the deformation of stationary and moving ferrofluid marbles in the presence of a permanent magnet. In the stationary case, the radius of the contact area scales with the fourth root of the magnetic Bond number, while the height scales with the inverse square root of this number. This behavior is similar to that of a marble with a puddle shape in the absence of the magnet versus its respective Bond number. The motion of a marble dragged by a permanent magnet leads to further deformation. A simple scaling analysis shows that the dimensionless change in curvature is proportional to the capillary number. Experimental results indicate that the dimensionless height and the dimensionless contact diameter of the marbles do not depend significantly on the speed or the capillary number. Similar to the stationary case, these geometric parameters are governed mainly by the magnetic Bond number. The present experiments cannot verify the scaling relationship between the deformation and the magnetic Bond number. A better experiment design that can isolate the influences of gravity, marble volume and magnetic field strength would be needed. Better data can also be obtained with a more accurate measurement of the magnetic flux density and magnetization density. The insights gained from the present work are valuable for the selection of the right volume, the right magnet size and the right speed for a ferrofluid marble working as an actuating vehicle in digital microfluidics.

Corresponding Author

*Nam-Trung Nguyen

Queensland Micro and Nanotechnology Centre, Griffith University, Brisbane, 4111, Australia.

Tel: +61 (07) 373 53921

Fax: (+61 07) 373 58021

Email: nam-trung.nguyen@griffith.edu.au

REFERENCES

(1) Nguyen, N.T. Micro magnetofluidics - interactions between magnetism and fluid flow on the microscale *Microfluid. Nanofluid.* **2012**, 12, 1-16.

(2) Nguyen, N.T.; Zhu, G.P.; Chua, Y.C.; Phan, V.N.; Tan, S.H. Magnetowetting and sliding motion of a sessile ferrofluid droplet in the presence of a permanent magnet, *Langmuir* **2010**, 26, 12553-12559

(3) Koh, W.H.; Lok, K.S.; Nguyen, N.T. A digital micro magnetofluidic platform for lab-on-a-chip applications *J. Fluid. Eng.-T ASME* **2013**, 135, 021302

(4) Mahadevan, L.; Pomeau, Y. Rolling droplets *Phys. Fluids* **1999**, 11, 2449-2453

(5) Aussillous, P. ; Quere, D. Liquid marbles *Nature* **2001**, 411, 924-927

(6) McEleney, P.; Walker, G.M.; Larmour, I. A.; Bell, S. E. J. Liquid marble formation using hydrophobic powders *Chem. Eng. J.* **2009**, 147, 373-382.

(7) Aussillous, P.; Quere, D. Properties of liquid marbles *P. R. Soc. A* **2006**, 462, 973-999.

(8) Bormashenko, E.; Pogreb, R.; Whyman, G.; Musin, A. Surface tension of liquid marbles *Colloid. Surface. A* **2009**, 351, 78-82.

(9) Bormashenko, E; Musin, A.; Whyman, G.; Barkay, Z.; Starostin, A.; Valtsifer, V.; Strelnikov, V. Revisiting the surface tension of liquid marbles: Measurement of the effective

surface tension of liquid marbles with the pendant marble method *Colloid. Surface. A* **2009**, 351, 78-82

(10) Arbatan, T.; Shen, W. Measurement of the surface tension of liquid marbles *Langmuir* **2011**, 27, 12923-12929

(11) Dorvee, J.R.; Derfus, A.M.; Bhatia, S.N.; Sailor, N.J. Manipulation of liquid droplets using amphiphilic, magnetic one-dimensional photonic crystal chaperones *Nat. Mater*. **2004**, 3, 896-899

(12) Zhang, L.B.; Cha, D.K.; Wang, P. Remotely Controllable Liquid Marbles *Adv. Mater.* **2012**, 24, 4756-4760

(13) Xue, Y.H.; Wang, H.X.; Zhao, Y.; Dai, L.M.; Feng, L.F.; Wang, X.G.; Lin, T. Magnetic liquid marbles: a "precise" miniature reactor *Adv. Mater*. **2010**, 22, 4814-4818

(14) Zhao, Y.; Xu, Z.G.; Parhizkar, M.; Fang, J.; Wang, X.G.; Lin, T. Magnetic liquid marbles, their manipulation and application in optical probing *Microfluid. Nanofluid.* **2012**, 13, 555-564

(15) Bormashenko, E.; Pogreb, R.; Bormashenko, Y.; Musin, A.; Stein, T. New Investigations on Ferrofluidics: Ferrofluidic marbles and magnetic-field-driven drops on superhydrophobic surfaces *Langmuir* **2008**, 24, 12119-12122

(16) Zhu, G.P; Nguyen, N.T.; Ramanujan, R.; Huang, X.Y. Nonlinear deformation of a ferrofluid droplet in a uniform magnetic field *Langmuir*, 2011, **27**, 14834-14841

(17) Afkhami, S.; Renardy Y.; Renardy M.; Riffle J. S.; Pierre T. S. Field-induced motion of ferrofluid droplets through immiscible viscous media *J. Fluid Mech.*, 2008, **610**, 363-380

(18) Afkhami, S.; Tyler, Y.; Renardy Y., Pierre T. S.; Woodward, R.; Riffle J. S. Deformation of a hydrophobic ferrofluid droplet suspended in a viscous medium under uniform magnetic fields *J. Fluid Mech.*, 2010, **663**, 358-384

(19) Timonen, J. V. I.; Latikka, M.; Leibler, L.; Ras, R. H. A.; Ikkala, O. Switchable static and dynamic self-assembly of magnetic droplets on superhydrophobic surfaces *Science*, 2013, **341**, 253-257

(20) Piroird, K.; Texier, B.D.; Clanet, C.; Quéré D. Reshaping and capturing Leidenfrost droplets with a magnet *Phys. Fluids*, 2013, **25**, 032108

(21) Bormashenko, E.; Pogreb, R.; Balter, R.; Gendelman, O.; Aurbach, D. Composite non-stick droplets and their actuation with electric field *Appl. Phys. Let.*, 2012, **100**, 151601